RESEARCH ACTIVITIES VIII
Laser Research Center for Molecular Science

VIII-A Developments and Researches of New Laser Materials

Although development of lasers is remarkable, there are no lasers which lase in ultraviolet and far infrared regions. However, it is expected that these kinds of lasers break out a great revolution in not only the molecular science but also in the industrial world.

In this project we research characters of new materials for ultraviolet and far infrared lasers, and develop new lasers by using these laser materials.

VIII-A-1 High-Energy, All-Solid-State, Ultraviolet Laser Power-Amplifier Module Design and Its Output-Energy Scaling Principle

ONO, Shingo; SUZUKI, Yuji; KOZEKI, Toshimasa; MURAKAMI, Hidetoshi; OHTAKE, Hideyuki; SARUKURA, Nobuhiko; SATO, Hiroki[1]; MACHIDA, Susumu[1]; SHIMAMURA, Kiyoshi[1]; FUKUDA, Tsuguo[2]
([1]Tokin Corp.; [2]Tohoku Univ.)

[*Appl. Opt.* **41**, 7556 (2002)]

We demonstrated that a coaxially pumped, large-aperture ultraviolet power-amplifier module using solid-state tunable laser medium Ce^{3+}:$LiCaAlF_6$ has 98-mJ, 290-nm, and 3-ns output pulses with sufficient extraction efficiency of 25%. The detailed information of design parameters, including the gain-coefficient dependence on pump condition, is successfully accumulated for further energy scaling for a terawatt-class ultraviolet chirped pulse amplification laser system or a high-pulse-energy laser system.

VIII-A-2 Generation of Intense 25-fs Pulses at 290 nm by Use of a Hollow Fiber Filled with High-Pressure Argon Gas

LIU, Zhenlin[1]; ONO, Shingo; KOZEKI, Toshimasa[2]; SUZUKI, Yuji[2]; SARUKURA, Nobuhiko[2]; HOSONO, Hideo[1,3]
([1]ERATO; [2]IMS, ERATO; [3]Tokyo Inst. Tech.)

[*Jpn. J. Appl. Phys.* **41**, L986 (2002)]

Frequency-tripled pulses at 290 nm from a 100-fs, 1-kHz Ti:sapphire regenerative amplifier system are spectrally broadened in hollow fiber filled with high-pressure argon gas. The self-phase-modulated pulses are compressed to 25 fs through a prism pair. The compressed pulse has an energy of 15 μJ.

VIII-A-3 Anomalous Power and Spectrum Dependence of THz Radiation from Femtosecond-Laser-Irradiated InAs in a High Magnetic Field of 14 T

OHTAKE, Hideyuki; MURAKAMI, Hidetoshi; YANO, Takayuki; ONO, Shingo; SARUKURA, Nobuhiko; TAKAHASHI, Hiroshi[1]; SUZUKI, Yuji[1]; NISHIJIMA, Gen[2]; WATANABE, Kazuo[2]
([1]GUAS; [2]Tohoku Univ.)

[*Appl. Phys. Lett.* **82**, 1164 (2003)]

We report on the THz radiation from femtosecond-laser-irradiated InAs in a high magnetic field up to 14 T. It is found that the radiation power exhibits anomalous magnetic-field dependence, including saturation, decrease, and recovery up to 14 T. Moreover, the radiation spectrum possesses a clear periodic structure over 6 T, possibly due to differently phased radiation from holes with different masses.

VIII-A-4 Significant Enhancement of Terahertz Radiation from InSb by Use of a Compact Fiber Laser and an External Magnetic Field

TAKAHASHI, Hiroshi[1]; SUZUKI, Yuji[1]; SAKAI, Masahiro; ONO, Shingo; SARUKURA, Nobuhiko; SUGIURA, Toshiharu[2]; HIROSUMI, Tomoya[2]; YOSHIDA, Makoto[2]
([1]GUAS; [2]Aisin Seiki Co., Ltd.)

[*Appl. Phys. Lett.* **82**, 2005 (2003)]

We investigated the magnetic-field dependence of terahertz (THz) radiation power from InSb. Significant enhancement of THz-radiation power is observed by using a compact fiber laser that delivered 100 fs optical pulses at a center wavelength of 1560 nm. Additionally, applying external magnetic fields dramatically enhanced the THz-radiation power. THz-radiation power reaches a maximum value at around 1.2 T, and its enhancement factor exceeds 100. From an applications viewpoint, this is a significant finding for practical light source design, since it is easily achieved by using a compact fiber laser and a conventional magnet.

VIII-A-5 Micro-Character Printing on a Diamond Plate by Femtosecond Infrared Optical Pulses

TAKESADA, Masaki[1,2]; VANAGAS, Egidijus[3]; TUZHILIN, Dmitri[3]; KUDRYASHOV, Igor[3]; SURUGA, Shoji[3]; MURAKAMI, Hidetoshi; SARUKURA, Nobuhiko; MATSUDA, Kazunari[1]; MONONOBE, Shuji[1]; SAIKI, Toshiharu[1]; YOSHIMOTO, Mamoru[4]; KOSHIHARA, Shin-ya[1]

([1]KAST; [2]Hokkaido Univ.; [3]Tokyo Instrument Inc.; [4]Tokyo Inst. Tech.)

[*Jpn. J. Appl. Phys.* **42**, 4613 (2003)]

Processing of less than 400 nm has been performed on the surface of a diamond plate by means of a femtosecond infrared pulse laser. Various characters with a size of about 1 μm were drawn by the femtosecond pulse laser system in conjunction with a microscope equipped with a precisely controlled piezo-stage. The tightly focused laser light on the flat surface of the diamond made it possible to minimize the light-induced graphitization. The surface of the diamond plate after laser machining was analyzed by micro-Raman measurements to estimate the graphitization effect induced by laser irradiation. The obtained results indicate that graphitization increased with the number of irradiated laser pulses.

VIII-A-6 Mode-Locking Stability Adjustment of a Kerr-Lens Mode-Locked Ti:sapphire Laser, Analyzed by a Recently Developed Real-Time Spectrum Analyzer

TAKAHASHI, Hiroshi[1]; SUZUKI, Yuji[1]; MURAKAMI, Hidetoshi; ONO, Shingo; SARUKURA, Nobuhiko; NAKAMURA, Tadashi[2]
([1]GUAS; [2]Textronix Japan., Ltd.)

[*Jpn. J. Appl. Phys.* **42**, 4330 (2003)]

This is a report on the mode-locking stability of a Kerr-lens mode-locked Ti:sapphire, measured by a newly developed noise measurement method. Mode-locking stability is monitored *via* a power spectrum, which is obtained by irradiating optical pulses onto a fast photodiode, and by processing the detected signal using a recently developed real-time spectrum analyzer. The mode-locking stability of the Ti:sapphire laser strongly depends on pump power and becomes unstable as pump power decreases from an optimum power level. Amplitude fluctuation and Q-switched mode-locking are notably observed as the main causes for a break in a continuous-wave (CW) mode-locking operation. Moreover, chaotic frequency hopping is observed in a Q-switched mode-locking operation. A real-time spectrum analyzer provides a time-varying power spectrum, which enables easy adjustment for stable CW mode-locking operation of ultra-fast solid state lasers.

VIII-A-7 Magnetic-Field-Induced Enhancement of THz-Radiation Power from Femtosecond-Laser-Irradiated InAs up to 27 T

TAKAHASHI, Hiroshi[1]; SUZUKI, Yuji[1]; QUEMA, Alex; SAKAI, Masahiro; YANO, Takayuki; ONO, Shingo; SARUKURA, Nobuhiko; HOSOMIZU, Masato[2]; TSUKAMOTO, Takeyo[2]; NISHIJIMA, Gen[3]; WATANABE, Kazuo[3]
([1]GUAS; [2]SUT; [3]Tohoku Univ.)

[*Jpn. J. Appl. Phys.* **42**, L532 (2003)]

Magnetic-field dependence of THz-radiation power from InAs surface is investigated by using a hybrid magnet, which is capable of providing a magnetic field up to 28 T. It is found that THz-radiation power saturates at around 3 T and also at 13 T. Maximum THz-radiation power with high-frequency component spectrum is observed at 3-T. This result leads to the conclusion that a magnetic field of 3 T is optimum for the enhancement of THz-radiation power. Additionally, THz-radiation spectrum exhibits periodic structure at magnetic fields above 12 T. This can be attributed to the change of dielectric constant induced by the strong magnetic field resulting in the interference of THz-radiation pulses from the front and back surfaces of the InAs substrate.

VIII-A-8 Optical Properties of Ce^{3+} Ion Doped $LiCaAlF_6$ Crystal in Vacuum Ultraviolet Region

TAKAHASHI, Hiroshi[1]; SAKAI, Masahiro; ONO, Shingo[1]; SARUKURA, Nobuhiko; SATO, Hiroki[2]; YOSHIKAWA, Akira[2]; FUKUDA, Tsuguo[1]
([1]GUAS; [2]Tohoku Univ.)

[*Jpn. J. Appl. Phys.* **42**, L660 (2003)]

The optical properties of Ce^{3+} ion doped $LiCaAlF_6$ (Ce:LiCAF) crystal is investigated in vacuum ultraviolet (VUV) region. It is found that the optical excitation from the valence band of LiCAF crystal to the highest ^2D excited state of Ce^{3+} can be utilized as an efficient excitation channel to obtain the ultraviolet emission due to $4f$–$5d$ transition of Ce^{3+}. Furthermore, the energy level of ^2D state is found to be located near the conduction band of LiCAF crystal, which leads to the electron transfer from the LiCAF crystal to the active Ce^{3+} ion.

VIII-A-9 Identification of Potential Estrogenic Environmental Pollutants by Terahertz Transmission Spectroscopy

QUEMA, Alex; TAKAHASHI, Hiroshi[1]; SAKAI, Masahiro; GOTO, Masahiro; ONO, Shingo; SARUKURA, Nobuhiko; SHIODA, Ryu[2]; YAMADA, Norihide[2]
([1]GUAS; [2]Agilent Tech. Res. Cent.)

[*Jpn. J. Appl. Phys.* **42**, L932 (2003)]

Using magnetically enhanced terahertz radiation from InAs, various naphthols, which exhibits estrogenic like activity and are potentially mimic natural hormones, are studied. The experimental results show that the naphthols, depicted by the position of the hydroxyl (-OH) component at different carbon atom sites of the naphthalene compound, are distinguishable based on the absorption of THz radiation. It is found that the THz radiation absorption is strongly related to the crystal symmetry and dipole moment of these isomers.

VIII-A-10 Excitation Fluence Dependence of Terahertz Radiation Mechanism from Femtosecond-Laser-Irradiated InAs under Magnetic Field

TAKAHASHI, Hiroshi[1]; QUEMA, Alex; YOSHIOKA, Ryoichiro; ONO, Shingo; SARUKURA, Nobuhiko
([1]GUAS)

[*Appl. Phys. Lett.* **83**, 1068 (2003)]

The excitation fluence and magnetic field dependence of terahertz (THz) radiation power from InAs is investigated. At low excitation fluence, an enhancement of the THz-radiation power is observed independent of the magnetic-field direction. As the excitation fluence is increased, a crossover of terahertz radiation mechanism is observed. At excitation fluence above this crossover, the radiation power is either enhanced or reduced depending on the magnetic-field direction. These results are explained by considering the different THz-radiation mechanisms from the InAs surface with or without photoexcited carrier screening.

VIII-B Development and Research of Advanced Tunable Solid State Lasers

Diode-pumped solid-state lasers can provide excellent spatial mode quality and narrow linewidths. The high spectral power brightness of these lasers has allowed high efficiency frequency extension by nonlinear frequency conversion. Moreover, the availability of new and improved nonlinear optical crystals makes these techniques more practical. Additionally, quasi phase matching (QPM) is a new technique instead of conventional birefringent phase matching for compensating phase velocity dispersion in frequency conversion. These kinds of advanced tunable solid-state light sources, so to speak "Chroma Chip Lasers," will assist the research of molecular science.

In this projects we are developing Chroma Chip Lasers based on diode-pumped-microchip-solid-sate lasers and advanced nonlinear frequency conversion technique.

VIII-B-1 Highly Efficient Continuous-Wave 946-nm Nd:YAG Laser Emission under Direct 885-nm Pumping

LUPEI, Voicu[1]; PAVEL, Nicolaie[2]; TAIRA, Takunori

([1]IAP-NILPRP, Romania; [2]IMS and IAP-NILPRP, Romania)

[*Appl. Phys. Lett.* **81**, 2677 (2002)]

The quasi-three-level 946-nm emission of Nd^{3+} in YAG is important for construction of low-heat solid-state lasers at fundamental frequency or for doubling it by nonlinear processes to blue 473-nm radiation. Successful attempts to lase the Nd:YAG at 946 nm in continuous-wave (CW) or pulsed regimes have been reported;[1)–3)] however, the performances of these lasers are still limited and the full lasing potential is not yet exploited. This paper discusses some possibilities to improve the laser emission parameters and to reduce the generation of heat by pumping directly into the emitting level.

In a CW quasi-three-level laser the fractional thermal loading η_h (*i.e.* the fraction of absorbed power that is transformed into heat by non-radiative processes), contains specific contributions from the ions that participate in the lasing process as well as from those that do not lase. The quantum defect ratio for the 946-nm laser emission is much larger than that corresponding to the fluorescence emission, whose average wavelength $\bar{\lambda}$ is 1038 nm. The contribution to heating from each excited Nd^{3+} ion that does not lase would be then much larger than from each ion that participate to lasing; thus, a high laser extraction efficiency will contribute to the reduction of the heat generated in the pumped laser material. A complex interrelation exists between the laser emission parameters and the heat generation and an optimization of all these characteristics would be necessary in order to make a complete use of the quasi-three-level emission potential. Both the laser emission parameters and the generation of heat are influenced by the quantum defect ratio $\eta_{qd} = \lambda_p/\lambda_l$ between the pump and laser emission wavelengths. Traditionally the 946-nm Nd:YAG lasers are pumped at 808 nm into the level $^4F_{5/2}$: this induces a parasitic upper quantum defect of ~1000 cm^{-1} between the pump and the emitting laser levels that accounts for more than half of the total quantum defect. As evidenced by the spectroscopic investigations[4)–6)] very suitable for diode laser pumping the Nd:YAG is the double-peaked absorption band centred around 885 nm that collects the thermally activated transitions $Z_2 \rightarrow R_1$ and $Z_3 \rightarrow R_2$ of the absorption spectrum $^4I_{9/2} \rightarrow {}^4F_{3/2}$. This wavelength of pump determines an increase of the quantum defect ratio by ~ 9.5%, leading to a corresponding improvement of the laser emission parameters. Moreover, by restricting strongly the reabsorption losses η_h could be diminished by as much as 50 to 60% from the value corresponding to that of 808-nm pumping.

The 946-nm CW emission in a 1.0-at.% Nd:YAG crystal (3-mm thick) is investigated by using 885-nm Ti:sapphire longitudinal pumping. The crystal was AR coated for 808 and 885 nm (reflectivity, $R < 0.5\%$), and also 946 and 1064 nm ($R < 0.1\%$). A plane-concave resonator of 25-mm length and output mirror of 50-mm radius was employed. The Ti:sapphire laser is focused on the Nd:YAG in a 160-μm diameter spot. The 946-nm laser output power *vs.* the absorbed power at 885 nm is shown in Figure 1. This dependence reflects the increase of the slope efficiency $\eta_s^{(a)}$ with increasing absorbed power, owing to the saturation of the reabsorption. The output power depends on *R*: a high reflectivity leads to a lower threshold but also to lower slope efficiency. The best results are obtained with $R = 97\%$ output mirror: the absorbed power at threshold is ~ 120 mW and $\eta_s^{(a)}$ at absorbed power about 4 times larger than the threshold reaches as much as 68%. Output power of 180 mW resulted for ~ 500 mW absorbed power at 885-nm. In our knowledge this is the largest slope efficiency obtained for CW 946-nm Nd:YAG laser emission. At $R = 93\%$ the threshold increases to ~ 260 mW, but $\eta_s^{(a)}$ at pump ~ 2 times larger than the threshold is already 63%. For $R = 98.8\%$ $\eta_s^{(a)}$ was 47%, while the absorbed power at threshold was ~ 110 mW.

The 1064-nm emission at 885-nm pumping (Figure 2) gives $\eta_s^{(a)}$ of 72% and 30 mW absorbed power at threshold for a mirror with $R = 90\%$. Slope efficiencies of 64% and 31% were obtained for $R = 95$ and 99%, respectively, with absorbed pump power at threshold of ~ 13 and ~ 5 mW.

The laser emission at 946 nm and 1064 nm under 808-nm pumping shows similar trends. The highest $\eta_s^{(a)}$at absorbed power of ~ 4 times above the threshold, namely 48%, resulted for the $R = 93\%$ mirror; the threshold was ~ 300 mW and ~ 350 mW at 946 nm were obtained for an absorbed power of ~ 1.3 W. For *R*

= 97% $\eta_s^{(a)}$ = 45% and the threshold was ~ 200 mW, while for R = 98.8% these parameters were 24% and ~ 145 mW. The 1064-nm emission had slopes of 12%, 42%, 51% for the output mirror with R = 99, 95, and 90%, respectively, while the 808-nm power absorbed at threshold was 16, 26, and ~ 45 mW. It can be observed that under 808-nm pumping the emission threshold is larger and $\eta_s^{(a)}$ is smaller than for 885-nm pumping.

Pumping resonantly into the emitting level can sensibly enhance the laser emission parameters in absorbed power. However, the weaker absorption at 885 nm as compared to 808 nm for a component of given length could reverse the situation when the laser parameters are expressed in input power. Lengthening the active component in order to increase the pump absorption will increase the reabsorption losses. A suitable solution for increasing the absorption could be a decoupling of the lengths for pump absorption from that of reabsorption, which can be achieved in a laser configuration with multi-pass of the pumping radiation inside the laser component.[7] The use of more concentrated Nd:YAG components in such a multi-pass laser configuration could also improve the absorption. Once the reabsorption becomes very low, the effect of reduction of the emission quantum efficiency by concentration quenching on threshold in these materials could be completely compensated by the increased pump absorption efficiency, similar to the 1064-nm Nd:YAG lasers. Further calculation shows that in a multi-pass laser cavity the laser parameters in input power under 885 and 808-nm pumping are similar. Such multi-pass 885-nm pumped 946-nm Nd:YAG lasers would enable an optimum use of pump power, resulting in superior laser performances and low heat generation that could enable the scaling to higher powers.

References

1) T. Y. Fan and R. L. Byer, *J. Opt. Soc. Am. A* **3**, 109 (1986).
2) G. Holleman, E. Piek and H. Walther, *Opt. Lett.* **19**, 192 (1994).
3) P. Zeller and P. Peuser, *Opt. Lett.* **25**, 34 (2000).
4) R. Lavi and S. Jackel, *Appl. Opt.* **39**, 3093 (2000).
5) V. Lupei, A. Lupei, N. Pavel, T. Taira, I. Shoji and A. Ikesue, *Appl. Phys. Lett.* **79**, 590 (2001).
6) V. Lupei, A. Lupei, S. Georgescu, T. Taira, Y. Sato and A. Ikesue, *Phys. Rev. B* **64**, 092102 (2001).
7) A. Giesen, H. Hugel, A. Voss, K. Wittig, U. Braud and H. Opower, *Appl. Phys. B* **58**, 365 (1994).

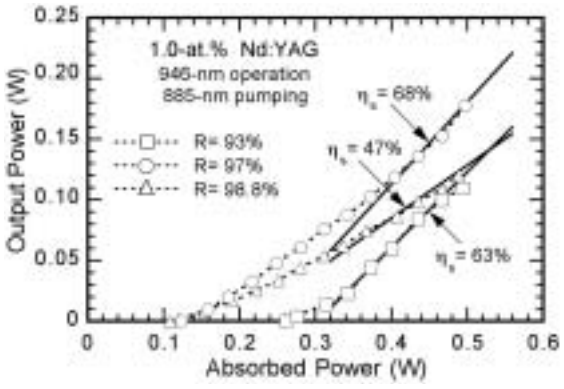

Figure 1. Output power at 946 nm function of the absorbed power under 885-nm Ti:Sapphire pumping.

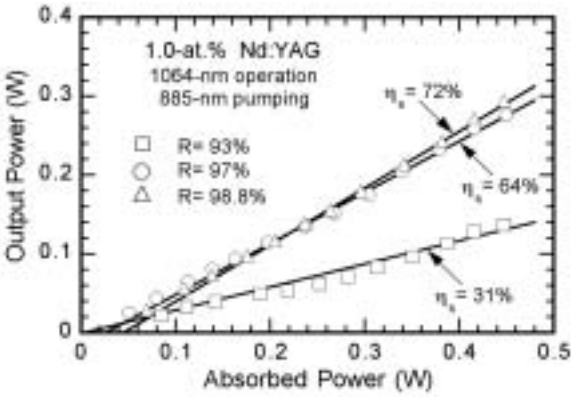

Figure 2. 1064-nm output power versus the absorbed power under 885-nm Ti:Sapphire pumping.

VIII-B-2 100-W Quasi-Continuous-Wave Diode Radially Pumped Microchip Composite Yb:YAG Laser

DASCALU, Traian[1,2,3]; TAIRA, Takunori; PAVEL, Nicolaie[2,3]

([1]CREATE-Fukui, Japan; [2]IAP-NILPRP, Romania; [3]IMS)

[*Opt. Lett.* **27**, 1791 (2002)]

The diode-pumped Yb:YAG medium has been demonstrated as a good candidate for high-power 1-μm laser systems as well as for tunable, single-axial-mode microchip configurations.[1)–3)] Besides of choice of gain medium, the configuration used for pumping, cooling and extraction plays a critical role in power scaling of a microchip laser. Recently, for scaling of a microchip Yb:YAG laser we proposed a new geometry that consists of a diode radial pumped composite Yb:YAG microchip.[4)] Theoretically was concluded that an output power of 100 W with overall optical-to-optical efficiency η_o of 39% could be obtained, employing an 13-at.% Yb-doped core of 2-mm diameter. Here we report first experimental results on this configuration: under quasi-continuous-wave (CW) pumping the best results of 112-W peak output power with η_o = 38% and slope efficiency in input power η_s of 63% were obtained.

The configuration of the diode radial pumped Yb:YAG microchip laser is shown in Figure 1. The composite crystal consists of a Yb:YAG doped core of square shape and that is diffusion bonded to an undoped YAG region. One side of the crystal was high reflectivity (HR) coated at the laser wavelength while the other surface was AR coated for this wavelength. The crystal is mounted with its HR coated side on a microchannel cooling system (water flow type, 20 °C temperature) and an indium based soldering technique was used to decrease the thermal impedance between them. The crystal was pumped by two JOLD-100-CAXF-15A diode fiber-coupled lasers (JenaOptik, Laserdiode GmbH, Germany) that delivers, each one, ~ 120 W maximum power at 940 nm ($\Delta\lambda$ ~ 4.0 nm FWHM) through a fiber of 0.6-mm core diameter and NA = 0.22. The pumping light was focused on the edge of the undoped YAG with a 1:1 achromatic optical system. Inside of the microchip it propagates by total

internal reflection through the Yb-doped core where is partially absorbed. The remained light propagates until it reaches the other edge of the undoped YAG slab: part of this light will be lost through the pumping window placed at that side, while the left light is scattered back into the microchip by a diffuse reflector.

Two crystals, one with core of 10-at.% Yb-doping level and 2 × 2-mm^2 square shape (sample #A) and the second of 1.2 × 1.2 mm^2 square 15-at.% Yb-doped core (sample #B) were used under a two diode lasers pumping, as in Figure 1. The slab shapes of 5-mm width and 0.8-mm thickness were obtained by cutting them from a 10-mm diameter rod.

The output *vs.* input power characteristics for these two crystals are presented in Figure 2, under quasi-CW pumping with rectangular pulses of 5 Hz repetition rate and 2.5% duty factor (pumping pulses of 5-ms duration). As output coupler a concave mirror of 0.1-m radius, placed 50-mm apart of the active medium, was employed. When the crystal #A is used with an output mirror of 97% reflectivity (R) a maximum output peak power of 66 W resulted at 220-W pumping power (Figure 2a); η_s was 49% (~ 58% in absorbed power). With an output mirror of R = 90% the threshold increases at ~ 33 W, however with an improved η_s of 54% (~ 64% in absorbed power). When crystal #B with R = 97% mirror was used we obtained maximum 63-W peak power with ~ 20-W absorbed at threshold and η_s far above threshold of 41% (~ 52% in absorbed power), as presented in Figure 2b. With the output mirror of R = 90% the threshold increased at ~ 33 W while η_s = 43% (~ 54% in absorbed power). The quasi-CW pumping with pulses of several milliseconds duration reduces the heat load of the crystals. The pulse duration is, however, long compared to the time necessary for the laser emission to reach the steady-state behavior. The obtained results suggest, therefore, the performances that could be obtained in CW operation if the heat is efficiently removed.

The power scalability of this microchip laser was investigated by using a third diode, placed perpendicular to the pumping directions of the first two (the inset of Figure 3). Figure 3 shows the input peak power *vs.* of pump peak power for the plane-concave resonator with R = 97% output mirror. A maximum of 112-W peak power for 298-W pump power, with η_s = 63%, was obtained for the crystal #B. For the crystal #A maximum peak power was 100 W and η_s was determined as 53%.

A future objective of this research is to demonstrate high-duty cycle or CW operation of Yb:YAG composite microchip by using this pumping scheme. As a first evaluation, the pumping repetition rate was increased, while the pumping pulse duration was kept at 5 ms. When the repetition rate increases from 10, to 30 and 60 Hz, the maximum peak output power for 298-W peak pump power decreases from 98, to 89 and 74 W, respectively, while η_s reduces from 52%, to 46% and 32% (output mirror with R = 90%). As much as 23-W average output power was obtained for 90-W average pump power (60 Hz repetition rate, 0.3 duty cycle). The temperature of the upper surface crystal was below 70 °C during all these experiments. An attempt of CW operation delivers 7.5 W for a pump power of 90 W; at this point an increase of the crystal temperature beyond 120 °C was however observed.

In conclusion a diode radial pumped composite Yb:YAG microchip laser is presented. Quasi-CW pumping of a 15-at.% Yb:YAG core (1.2 × 1.2 mm^2) with pulses of 5-Hz repetition rate and 2.5% duty cycle delivers 112-W peak power with 63% slope efficiency and 38% overall optical-to-optical efficiency. For further works, the temperature distribution into the Yb:YAG core was determined by a finite element method, while the output power was evaluated by taking into account the spatial variation of both the pump and the laser beams. The results show that efficient CW operation with 100-W power at room temperature could be obtained by using a 400-μm thick Yb:YAG chip and by improving the thermal impedance between the crystal and cooling head through an advanced soldering technique.

References

1) E. C. Honea, R. J. Beach, S. C. Mitchel, J. Skidmore, M. A. Emanuel, S. B. Sutton, S. A. Payne, P. V. Avizonis, R. S. Monroe and D. G. Harris, *Opt. Lett.* **25**, 805 (2000).
2) T. S. Rutherford, W. M. Tulloch, S. Sinha and R. L. Byer, *Opt. Lett.* **26**, 986 (2001).
3) T. Taira, J. Saikawa, T. Kobayashi and R. L. Byer, *IEEE J. Sel. Top. Quantum Electron.* **3**, 1000 (1997).
4) N. Pavel, J. Saikawa and T. Taira, *Jpn. J. Appl. Phys.* **40**, 146 (2001).

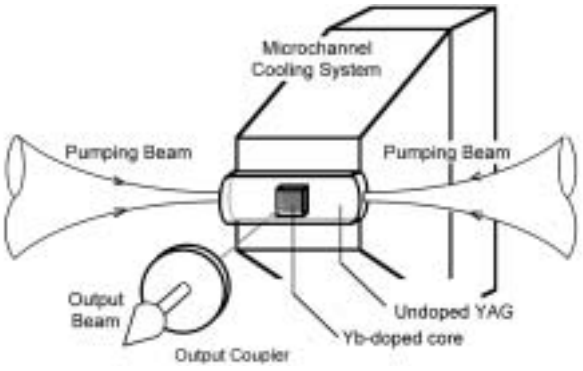

Figure 1. Schematic of the diode radial pumped composite Yb:YAG laser.

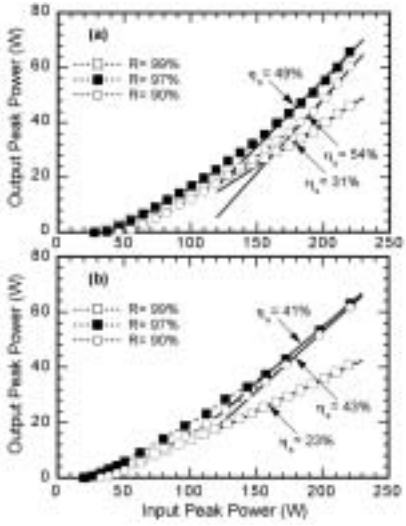

Figure 2. Output power *vs.* input power for composite Yb: YAG microchip laser with (a) crystal #A and (b) crystal #B.

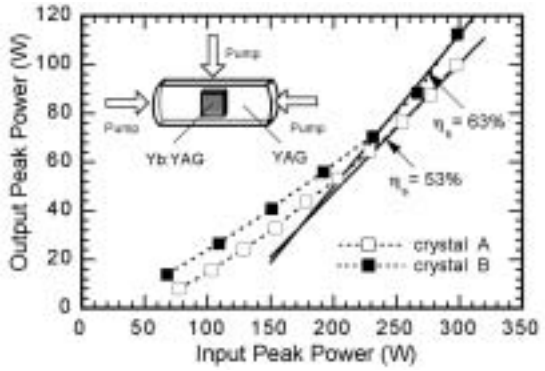

Figure 3. Performances of the microchip laser under pumping with three diodes, output coupler of 97% reflectivity.

VIII-B-3 Laser Operation with Near Quantum-Defect Slope Efficiency in Nd:YVO_4 under Direct Pumping into the Emitting Level

SATO, Yoichi; TAIRA, Takunori; PAVEL, Nicolaie[1]; LUPEI, Voicu[2]
([1]IMS and IAP-NILPRP, Romania; [2]IAP-NILPRP, Romania)

[*Appl. Phys. Lett.* **82**, 844 (2003)]

Construction of efficient solid-state lasers requires laser components able to absorb completely the pump radiation and to use it for high performance laser emission. These requirements are fulfilled by laser materials with broad and intense absorption bands that match the diode lasers emission spectrum, as well as with a high value for the product of the effective emission cross section σ_{eff} and the effective luminescence lifetime $\tau_f = \tau_{rad}\eta_{qe}$, where η_{qe} is the emission quantum efficiency. The Nd-doped crystals of the vanadate family, such as YVO_4 or $GdVO_4$, fulfill well these spectroscopic requirements.[1),2)] The Nd:YVO_4 lasers are traditionally pumped into the strongly absorbing $^4F_{5/2}$ level at 808.8 nm and this introduces a parasitic upper quantum defect (QD) between the pumping- and the emitting-laser level. The global QD in these lasers could be then reduced by elimination of this upper QD by pumping directly into the emitting level $^4F_{3/2}$. This modality of pumping was used in the first experiments to demonstrate the possibility of excitation of Nd^{3+} emission by resonant diode pumping.[3)] Recently, the pumping into the emitting level was reinvestigated for diluted Nd:YVO_4 crystals;[4)–6)] preliminary data on concentrated Nd:YVO_4 crystals were also reported.[5),6)] It was thus revealed that a suitable pump transition for Nd:YVO_4 is $^4I_{9/2}(Z_1) \rightarrow {}^4F_{3/2}(R_1)$, at 879.8 nm. The slope efficiency of the 1064-nm laser emission for both 809 and 880-nm pump was lower than the limit determined by η_{qd} for these wavelengths (0.760 and 0.827, respectively), even considering fairly large residual optical losses *L*. While for direct pumping this difference can be attributed[5),6)] to a less than unity efficiency of superposition between the pump and laser volumes η_m and to the use of uncoated crystals, in case of 809-nm pumping the possibility of a less than unity of η_p must be further checked. The aim of the present work is the improvement of laser parameters by using coated crystals and pump focusing conditions able to increase η_m. A method to determine the pump level efficiency η_p for 809-nm pumping based on pump saturation effects was developed.

The 1-μm CW laser emission of Nd:YVO_4 was investigated under end-pumping with 880-nm radiation of a Ti:Sapphire and of a diode laser. The laser crystal was a 1.0-mm thick *a*-cut plate with 1.0-at.% Nd, AR coated on both sides for 809, 880 and 1064-nm wavelengths. A plane-concave resonator of 45-mm length and 50-μm radius of the output mirror was used under Ti:Sapphire pumping. The Gaussian pump light was focused on crystal in a 50-mm diameter spot and the excitation was made with $E \| c$ crystal axis. Figure 1 shows the output power *vs.* Ti:Sapphire 880-nm input power. For a 10% transmission (T) output coupler the slope efficiency reached 80%, the threshold of emission was ~ 25-mW and for 1.0 W input power the laser emitted 0.79 W at 1064 nm. Slope efficiency of 74% and 67% resulted with T = 5 and 3%, respectively. These data give consistently round-trip residual losses L of ~ 0.9 % with η_m close of unity, and thus the difference between the obtained slope efficiency and that determined by the QD for this wavelength of pump can be fully accounted by the residual optical losses L. When the Ti:Sapphire laser wavelength was tuned to 809 nm the slope efficiency in the range of 70 to 650 mW input power was 70%, 63% and 57% for T = 10%, 5% and 3%, respectively.

Traditionally, for 809-nm pumping η_p has been considered as unity;[7)] however, other laser emission results[8)] indicate a lower value (~ 0.95) that could be, however, influenced by uncertainties in determining η_m. Here we show that η_p can be evaluated independently based on saturation effects in the pump transmission. Based on a rate equation modeling that accounts for this emission, a general equation for the dependence of the pump power on the distance *z* inside the active medium in absence of laser emission was obtained:

$$\frac{dP_{in}(z)}{dz} = -\alpha_a \frac{\pi w_p^2 \cdot I_p^{sat}}{2\beta} \times \ln\left[1 + \frac{2\beta}{\pi w_p^2 \cdot I_p^{sat}} P_{in}(z)\right] \qquad (1)$$

where $P_{in}(z)$ is the pump power, I_P^{sat} is the pump-saturation intensity, α_a is the absorption coefficient, and w_p the pump beam waist. The parameter β accounts for the mechanisms of excitation and de-excitation of the emitting level: for pumping above the emitting level (including 809-nm pumping), $\beta \equiv \eta_p$ while when pumping into the emitting level $\beta = 1 + f_2/f_0$, with f_2 and f_0 the fractional thermal population of the Stark sublevels $^4F_{3/2}(R_1)$ and $^4I_{9/2}(Z_1)$, respectively. Considering the energy level diagram of Nd:YVO_4 at the room temperature $f_0 = 0.4$, $f_2 = 0.52$ and $\beta = 2.3$.

Equation (1) integrated over the length of the crystal was used to estimate the parameter β from the fit of the measured transmission at various pump powers. In the experiments on saturation the Gaussian Ti:Sapphire radiation was focused on the 1-at.% Nd:YVO_4 crystal to a waist of 21-μm in case of 880 nm and 29-μm for 809-nm pumping. The absorption coefficients at 880 nm and

809 nm wavelengths, determined for low intensity of the Ti:Sapphire laser, were ~ 55 cm^{-1} and ~ 75 cm^{-1} respectively. In case of 809-nm pumping a good agreement was obtained for η_p = 1 (Figure 2); the inset of Figure 2 shows clearly the differences between the theoretical curves for η_p = 0.95 and 0.9 and the experimental data. At 880-nm pumping the effect of the induced emission on transmitted power at high pump intensity is evidenced by the good fit with β = 2.3.

A fiber array packed diode bars FAP-81-16C-800B laser (Coherent Co.) was next used to pump the Nd:YVO_4 crystal, in a 50-mm plane-plane resonator. A slope efficiency of 75% was obtained for T = 10% ($E||c$ pumping); the absorbed power at threshold was 0.55 W and 1.1-W output power resulted for 2.0-W absorbed power. The threshold absorbed power decreases to 0.33 and 0.16 W for T = 5 and 1%, respectively, however with a reduced slope efficiency of 69% and 28%.

In conclusion, one-micron highly efficient laser emission with 80% slope efficiency (~ 0.79 optical-to-optical efficiency) under Ti:sapphire and 75% slope efficiency relative to absorbed power under diode laser 880-nm pumping was obtained in a 1-mm thick, 1-at.% Nd:YVO_4 crystal; the first of these is close to the quantum defect limit. The pump-beam saturation effects on transmitted power under non-lasing condition indicate that η_p of the $^4F_{5/2}$ level is ~ 1.0. Directly-pumped highly Nd-doped vanadates have potential for construction of highly-efficient CW miniature lasers by using thinner active components with enhanced absorption and with extended capabilities to dissipate the heat or for scaling to higher powers; they could be also useful in the design of transversely-pumped Nd:YVO_4 lasers.

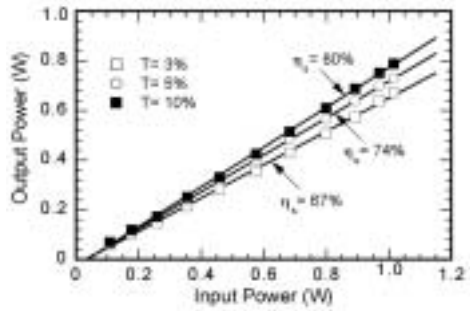

Figure 1. CW 1064-nm laser emission under 880-nm Ti:Sapphire pumping for 1-at.% Nd:YVO_4.

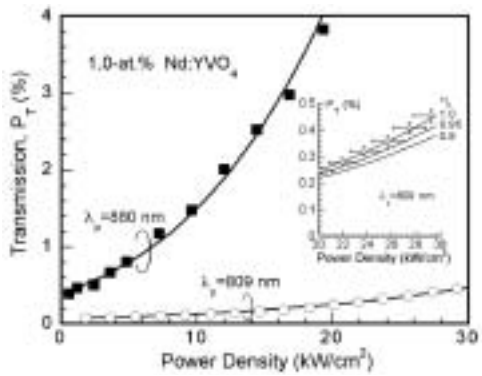

Figure 2. Transmitted power P_T *vs.* pump-beam intensity in absence of laser emission: symbols for experiments and curves from theory with β = 2.3 (880 nm) and η_p = 1 (809-nm pumping). The inset shows the fit of the 809-nm pump data with η_p = 1, 0.95, and 0.9.

References

1) R. A. Fields, M. Birnbaum and C. L. Fincher, *Appl. Phys. Lett.* **51**, 1885 (1987).
2) T. Jensen, V. G. Ostroumov, J. P. Meyn, G. Huber, A. I. Zagumennyi and I. A. Shcherbakov, *Appl. Phys. B* **58**, 373 (1994).
3) R. Newman, *J. Appl. Phys.* **34**, 437 (1963).
4) R. Lavi, S. Jackel, Y. Tzuk, M. Winik, E. Lebiush, M. Katz and I. Paiss, *Appl. Opt.* **38**, 7382 (1999).
5) V. Lupei, N. Pavel and T. Taira, *Opt. Commun.* **201**, 431 (2002).
6) V. Lupei, N. Pavel and T. Taira, *IEEE J. Quantum Electron.* **38**, 240 (2002).
7) A. W. Tucker, M. Birnbaum, C. L. Fincher and J. W. Erler, *J. Appl. Phys.* **48**, 4907 (1977).
8) R. A. Fields, T. S. Rose, M. E. Innochenzi, H. T. Yura and C. L. Fincher, *Proc. Advanced Solid State Lasers Conf.* (Optical Society of America, Washington, D.C.), 301 (1989).

VIII-B-4 High-Power Blue Generation in a Periodically Poled MgO:$LiNbO_3$ Ridge-Type Waveguide by Frequency Doubling of a Diode End-Pumped Nd:YAG Laser

PAVEL, Nicolaie[1]; SHOJI, Ichiro; TAIRA, Takunori; IWAI, Makato[2]; YOSHINO, Takeshi[2]; YAMAGUCHI, Shoichiro[2]; IMAEDA, Minoru[2]
([1]IMS and IAP-NILPRP, Romania; [2]NGK)

[*OSA, TOPS* **83**, 388 (2003)]

The $^4F_{3/2} \rightarrow {}^4I_{9/2}$ laser transition at 946 nm of Nd^{3+}:YAG opens the way for generation of continuous wave (CW) blue laser radiation that is of interest for various application, such us display technologies, obtaining of high-density optical disk systems, high-resolution printing, or biological applications. An attractive way to obtain a compact blue-light source is second-harmonic generation (SHG) by quasi-phase matching (QPM) interaction. Recently, MgO:$LiNbO_3$ (MgO:LN) was demonstrated to be a good nonlinear material for blue SHG: it presents higher resistance to photorefractive damage than LN, decreased coercive field compared with LN and a large nonlinear coefficient d_{33} ~ 25 (±2.5) pm/V.[1),2)] The key points for obtaining efficient and high-power SHG waveguide devices include strong confinement of the light wave into the waveguide, good overlap of fundamental and second-harmonic modes, prevention of nonlinear properties degradation, and maintaining of a high

optical-damage resistance, particularly in the shorter wavelength region. A CW blue power of 17.3 mW at 426 nm was demonstrated from a AlGaAs laser diode of 55-mW output power by using a MgO:LN proton-exchanged waveguide.[3] Proton-exchanged waveguides has, however some limitations, such as mode-field mismatching caused by dispersion and refractive index profiles, a trade-off between index change and non-linearity[4] and even degraded nonlinear properties.

A machining technique for processing three-dimensional waveguides[5] leads to a new waveguide technology: thus, a ridge-type waveguide QPM-SHG MgO:LN device that preserves the original performances of the nonlinear crystal was developed. CW SHG generation with 100 mW power at 412 nm using a Ti:Sapphire laser as a pumping source and with 14 mW output under diode laser pumping were demonstrated.[6] This work reports on our efforts toward scaling blue light obtained by frequency-doubling from a periodically polled MgO:LN ridge-type waveguide: using a diode end-pumped Nd:YAG laser operating at 946 nm as a fundamental source the maximum CW blue-light was 189 mW with a conversion efficiency of 49%.

A sketch of the experimental set-up is presented in Figure 1. A homemade diode-end pumped Nd:YAG laser was used in experiments. The 3-mm thick Nd:YAG crystal (1.0-at.% doping level) was AR coated for 809, 946 and 1064 nm. A 400-μm diameter, 0.22 NA fiber-coupled diode (HLU32F600, LIMO Co., Germany) was used for CW pumping. A plane-concave resonator of 30-mm length and output mirror of 100-mm radius was employed. With an output mirror of 97% reflectivity at 946 nm the laser delivered a random polarised beam of maximum 3.7 W for an absorbed power of 9.5 W in a beam characterised by a M^2 factor of 2.5. The slope efficiency was 44% with respect to the absorbed pump power. A glass plate positioned at the Brewster angle was used in order to achieve a polarised beam. For an absorbed power at 809 nm of 4.2 W the output was 1.1 W in a Gaussian beam (M^2 = 1.05). The laser spectrum, which was investigated with an Advantest Q8384 Spectrum Analyser (0.01-nm resolution), was centred at 946.2 nm and presented four longitudinal modes.

A periodically poled MgO:LN ridge-type waveguide of 8.5-mm length was used in experiments. Both the input and output surfaces were cut at 10° and AR coated at 946 nm by a SiO_2 monolayer; no coating was provided for the 473-nm wavelength. The MgO:LN ridge-type waveguide was placed on an aluminum plate whose temperature was controlled with 0.1 °C accuracy. The 946-nm radiation was varied by a rotating polarizer and focused into the waveguide with a lens of 8-mm focal length and NA = 0.55. For comparison, a Ti:Sapphire laser (Spectra Physics, Model 3900S) whose beam was characterized by M^2 ~ 1.03, was also used to pump the MgO:LN waveguide. Figure 2 presents the 473-nm blue light characteristics as a function of the 946-nm power coupled into the waveguide. The maximum blue power under Nd:YAG laser pumping was 189 mW with a conversion efficiency of 49%. If the Fresnel losses on the waveguide exit face are considered the maximum internal blue-light power is ~ 219 mW, corresponding to a conversion efficiency of ~ 57%. The measured temperature bandwidth was ΔT = 2.3 °C, in very good agreement with the predicted theoretical value of 2.35 °C. Under pumping by Ti:Sapphire laser the maximum blue power at 473-nm was 104 mW (conversion efficiency of 48%); the results were comparable with those obtained under pumping by Nd:YAG laser. The conversion efficiency saturation was attributed to the absorption of both the blue and fundamental radiations into the waveguide. Thus a slightly decrease of the phase-matching temperature with increasing of the blue output power was observed.

In conclusion, blue-light generation from a periodically polled $MgO:LiNbO_3$ ridge-type waveguide by frequency doubling of a diode end-pumped Nd:YAG laser is reported. To the authors best knowledge this is the first demonstration of such a system. The output power at 473 nm of 189 mW (internal power of 219 mW) was obtained, indicating the potential for high-power SHG of the ridge-type waveguide fabricated by ultra-precision machining.

References

1) I. Shoji, T. Kondo, A. Kitamoto, M. Shirane and R. Ito, *J. Opt. Soc. Am. B* **14**, 2268–2294 (1997).
2) A. Kuroda, S. Kurimura and Y. Uesu, *Appl. Phys. Lett.* **69**, 1565–1567 (1999).
3) T. Sugita, K. Mizuuchi, Y. Kitaoka and K. Yamamoto, *Opt. Lett.* **24**, 1590–1592 (1999).
4) K. Mizuuchi, H. Ohta, K. Yamamoto and M. Kato, *Opt. Lett.* **22**, 1217–1219 (1997).
5) T. Kawaguchi, K. Mizuuchi, T. Yoshino, J. Kondo, A. Kondo, M. Imaeda and K. Yamamoto, *Technical Digest of ISOM 2000* p. 66.
6) T. Kawaguchi, T. Yoshino, J. Kondo, A. Kondo, S. Yamaguchi, K. Noda, T. Nehagi, M. Imaeda, K. Mizuuchi, Y. Kitaoka, T. Sugita and K. Yamamoto, *Technical Digest of CLEO 2001 Conference*, 6–11 May 2001, Baltimore, USA, paper CTuI6, pp. 141–142.

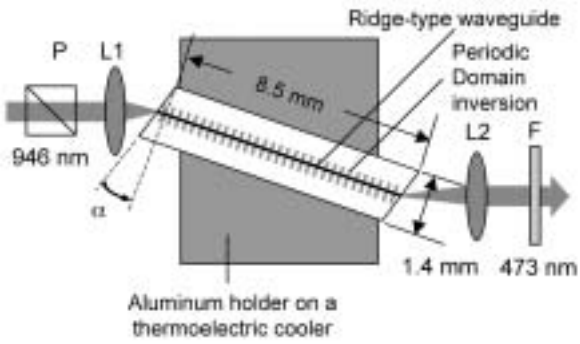

Figure 1. The experimental set-up for blue generation. P: polarizer; L1: focusing lens; L2: collimating lens; F: 946-nm cut filter.

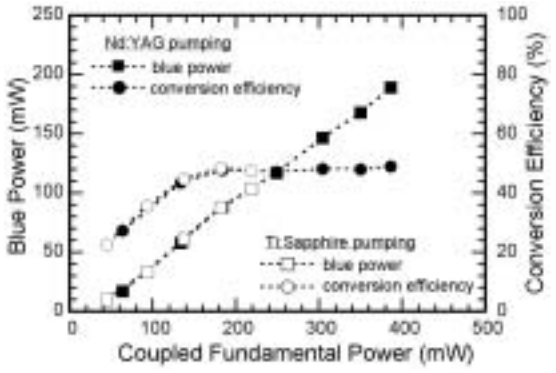

Figure 2. Blue laser characteristics vs. the 946-nm power coupled into the waveguide under pumping by Nd:YAG and Ti:Sapphire laser.

VIII-B-5 The Effect of Nd Concentration on Fundamental and Frequency-Doubled CW Laser Emission of Miniature Nd:YAG Lasers

LUPEI, Voicu[1]; PAVEL, Nicolaie[2]; TAIRA, Takunori
([1]IAP-NILPRP, Romania; [2]IMS and IAP-NILPRP, Romania)

[*CLEO/QELS 2003* paper CThM44]

This work discussed and demonstrated the benefit of using the direct pumping at 885 nm into the emitting level $^4F_{3/2}$ of concentrated Nd:YAG single crystals and ceramics for construction of efficient continuous-wave (CW) solid state lasers at the fundamental and frequency-doubled wavelength. Compared with the traditional 808-nm pumping into the strongly absorbing $^4F_{5/2}$ level, the direct pumping could improve the laser parameters (reduction of threshold and enhancement of slope efficiency) by ~ 10%, while the fraction of absorbed power transformed into heat for the 1064-nm laser emission can be diminished by ~ 30%. The reduced pump absorption of the emitting level can be compensated by using concentrated laser materials.[1)]

The laser components used in this investigation are 3-mm long Nd:YAG crystals with 1.0 or 2.4-at.% Nd and ceramics with 3.5-at.% Nd, coated as AR for 946 and 1064 nm and HT for the 808 and 885-nm wavelengths of pumping. The Gaussian radiation from a Ti:Sapphire laser was focused to a 50-μm diameter spot on the surface of the active media, for both pumping wavelengths. A plane-concave resonator of 35-mm length and output mirror of 50-mm radius was used for 1064-nm emission.

With an output mirror of 90% reflectivity the slope efficiency for the 1.0-at.% Nd sample under 885-nm pumping was 79%, close to the quantum defect limit of 83% (Figure 1). This is the largest slope efficiency reported so far for the CW Nd:YAG lasers. With increasing Nd concentration, C_{Nd} the slope efficiency diminishes slightly owing to increased residual losses: the value was 70% and 57% for the 2.4 and 3.5-at.% Nd:YAG, respectively. For the 808-nm pumping the slope efficiency for the 1.0, 2.4 and 3.5-at.% Nd:YAG components was 69%, 64%, and 52%, respectively. The best optical-to-optical efficiency in input power for 885-nm pumping is obtained with the 3.5-at.% Nd:YAG, which shows the largest absorption efficiency, while for 808-nm pumping the best results are obtained with the 2.4-at% Nd sample for which the absorption efficiency is already close to the unity. In case of 946-nm emission (output mirror of 97% reflectivity), the slope efficiency in absorbed power for the 1.0 and 2.4-at.% Nd under 885-nm pumping was 66% and 42%, respectively, while under 808-nm pumping the slope efficiency was 55% and 37%. For this wavelength of operation the increased reabsorption precludes the use of higher C_{Nd} for the single pump-pass lasers. However, as the theoretical modeling show, the direct pumping of the 946-nm emission of concentrated Nd:YAG can be much more efficient in case of multiple-pass-pumping.

The increased emission parameters at the fundamental frequency under direct pumping are expected to influence the performances of the intracavity frequency-doubling devices, such as a reduction of emission threshold and a more pronounced dependence on the absorbed pump power.[2)] This is evidenced with a end-pumped V-type frequency-doubling device for the Nd:YAG 1064-nm emission using a nonlinear LBO crystal (type I, critical phase matching, 25 °C temperature operation). A marked enhancement of the 532-nm emission in absorbed power was observed for the 1-at.% Nd:YAG crystal (Figure 2a). However, for a given input power the performances with 809-nm pumping are superior, although a strong limiting is observed for high pump powers. The green emission parameters in input power under 885-nm pumping are improved by using higher C_{Nd}, such as 2.4-at.% Nd, owing to the increased pump absorption efficiency (Figure 2b).

In conclusion, highly efficient fundamental (up to 79% slope efficiency) and frequency-doubled continuous-wave laser emission of Nd:YAG crystals and ceramics of various Nd concentration under 885-nm direct pumping with Ti:Sapphire laser is demonstrated. These results demonstrate the utility of direct pump of concentrated Nd laser materials for construction of efficient CW Nd lasers at the fundamental or doubled frequency.

References

1) V. Lupei, N. Pavel and T. Taira, *IEEE J. Quantum Electron.* **38**, 240 (2002).
2) V. Lupei, G. Aka and D. Vivien, *Appl. Phys. Lett.* **81**, 811 (2002).

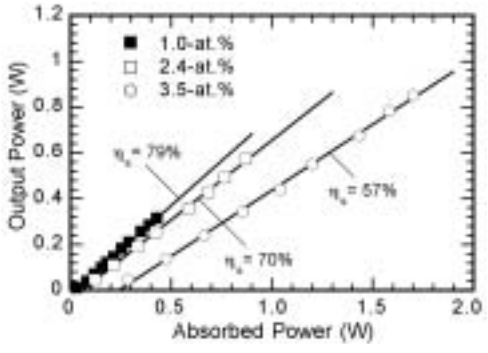

Figure 1. Output power at 1064 nm *vs.* absorbed power at 885-nm under Ti:Sapphire pumping.

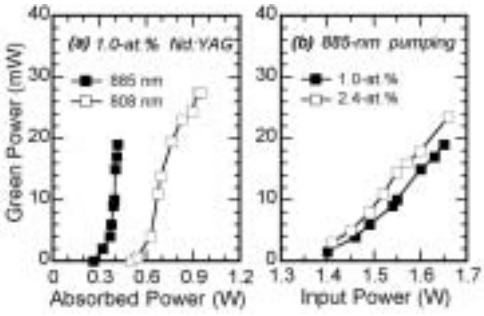

Figure 2. (a) Green power *vs.* absorbed power for the 1.0-at.% Nd:YAG crystal under 885 and 808-nm pumping, and (b) green power under 885-nm pumping for the 1.0 and 2.4-at.% Nd:YAG.

VIII-B-6 Great Reduction of Thermally-Induced-Birefringence Effect in Highly Nd^{3+}-Doped YAG Ceramics by Laser Oscillation

SHOJI, Ichiro; TAIRA, Takunori; IKESUE, Akio[1]; YOSHIDA, Kunio[2]
([1]JFCC; [2]Osaka Inst. Tech.)

[*CLEO/Europe* CA8-4-FRI (2003)]

Nd:YAG ceramics are promising materials for high-power and high-efficient microchip lasers because highly transparent and highly Nd^{3+}-doped ceramics are available with superior thermomechanical properties.[1)] We have investigated thermally-induced-birefringence effect in Nd:YAG ceramics and found that the depolarization loss of highly Nd^{3+}-doped ceramics is much larger than that of low-concentrated Nd:YAG single crystals even at the same absorbed pump power under non-lasing condition.[2)] This is mainly due to larger thermal loading, η_h, for higher Nd^{3+} concentration; η_h depends on the radiative quantum efficiency, η_r, which becomes smaller for higher Nd^{3+} concentration because of significant interaction between Nd^{3+} ions. Under lasing, however, η_h does not depend on η_r and then becomes a constant small value in an ideal case, reducing the depolarization to much smaller values than those under non-lasing. We experimentally investigated the reduction of depolarization under lasing condition.

The measurement was performed with the pump-probe measurement.[2)] A Ti:sapphire laser oscillating at 808nm was used as the pump source and a linearly polarized He-Ne laser was used as the probe. We used a 3.5at.% Nd:YAG ceramic, the thickness of which was 1.9mm, and also used a (111)-cut 3.0mm-thick 1.0at.% Nd:YAG single crystal as comparison. The laser output power as a function of the absorbed pump power for both the samples are shown in Figure 1. Lower output for the ceramic is supposed to be due to lower mode matching caused by more significant thermal-lens effect. Figure 2 shows the dependence of the depolarization on the absorbed pump power under non-lasing and lasing conditions. When lasing occurs, the depolarization of the 3.5at.% Nd:YAG ceramic reduced to 1/3 of that under non-lasing condition, which is nearly the same with that of the non-lasing single crystal. We also found that η_h is not constant even under lasing in a practical case, and the depolarization at each absorbed pump power can be estimated from the characteristics of the laser oscillation, as shown by the dotted curves in Figure 2.

In conclusion, we have experimentally verified that the depolarization of highly Nd^{3+}-doped YAG ceramics is greatly reduced by laser oscillation.

References

1) T. Taira, A. Ikesue and K. Yoshida, *OSA Trends in Optics and Photonics* **19**, 430 (1998).
2) I. Shoji, Y. Sato, S. Kurimura, V. Lupei, T. Taira, A. Ikesue and K. Yoshida, *Opt. Lett.* **27**, 234 (2002).

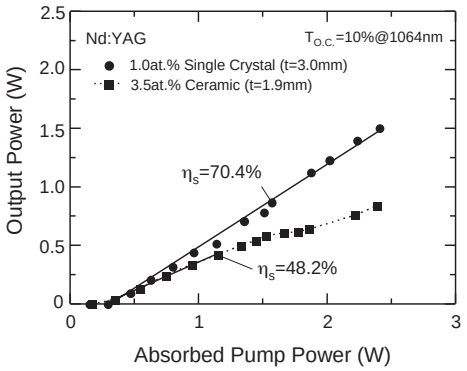

Figure 1. Laser output power as a function of the absorbed pump power for the ceramic and single-crystal.

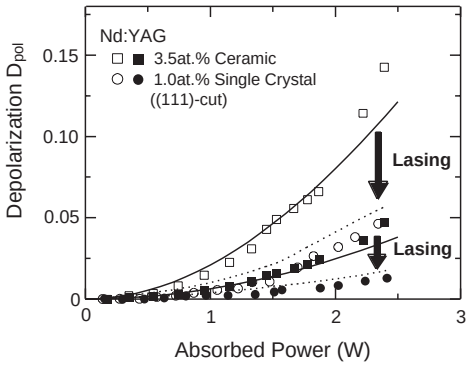

Figure 2. Dependence of the depolarization on the absorbed pump power under non-lasing and lasing conditions. The solid and dotted curves are the calculated depolarization under non-lasing and lasing conditions, respectively.

VIII-B-7 Periodical Poling Characteristics of Congruent MgO:$LiNbO_3$ Crystals at Elevated Temperature

ISHIZUKI, Hideki; SHOJI, Ichiro; TAIRA, Takunori

[*Appl. Phys. Lett.* **82**, 4062–4064 (2003)]

Quasi-phase matching (QPM) is an attractive technique for efficient nonlinear wavelength conversion, and various types of QPM devices have been demonstrated. A 5 mol% MgO-doped $LiNbO_3$ (MgO:LN) crystal has attracted much attention for the material of the QPM devices because of its higher resistance to photorefractive damage than that of non-doped LN. It has also a large nonlinear coefficient and a lower

coercive field to invert the sign of the nonlinear coefficient of the than that of non-doped LN. These features mean that MgO:LN is a suitable material for QPM devices with large cross-sections for high-power and/or short-pulse operation. However, few reports have been made on realizing bulk QPM devices by use of MgO:LN, and the maximum thickness was limited to 1mm. Here, we report the periodic poling characteristics of MgO:LN crystal at elevated temperature and demonstrate successful periodical poling of 3mm-thick MgO:LN crystals with 30 μm period.

The coercive field of MgO:LN was measured in an insulation-oil bath. An aluminum electrode of 0.2 μm thickness was prepared on the crystal surface by vacuum evaporation and photolithography. The measured coercive-field dependence on crystal temperature is shown in Figure 1. The open triangles are the estimated coercive field was measured by multipulse application totally longer than 100seconds, and the filled circles are the values obtained by applying only one high-field pulse of 1-second duration. The measured values by using 1-second pulse may have a little higher value than that by multipulse application because of the slow response time of the crystal. The coercive field decreased drastically with increasing temperature. The coercive fields at T = 250 °C were measured to be 1.2 kV/mm, which is about 1/4 compared with that for MgO:LN at room temperature(RT) and about 1/17 of that for non-doped LN at RT.

We tried to fabricate periodically poled structures of 30 μm grating period in 3-mm-thick MgO:LN at elevated temperature. At T = 170 °C, we achieved periodically poled structures with smooth surface by applying ~ 5 kV (~ 1.7 kV/mm) pulses as shown in Figure 2. Figure 2(a) shows the photograph of the *y*-face cross-section of obtained periodic structures after HF etching, and Fig. 2(b), 2(c) and 2(d) present the +*z* surface, *y*-face (expansion) and –*z* surface photographs, respectively. Periodic patterning with high aspect ratio (periodic-pattern width : crystal thickness) of 1:200 was realized.

In conclusion, we investigated the coercive field dependence on the crystal temperature for 5 mol% MgO:LN. The coercive field at 250 °C was found to reduce to about 1.2 kV/mm, which is about 1/4 of that at room temperature. We successfully fabricated periodic structures of 30 μm period with smooth surfaces in 3-mm-thick MgO:LN. The drastically reduced coercive field of MgO:LN crystals may enable us to realize much thicker QPM device than ever reported. This kind of thick QPM devices can be used as intracavity elements, and for high-power wavelength conversion, short-pulse amplification, and pulse compression.

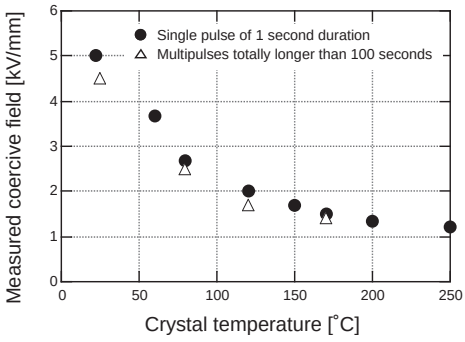

Figure 1.

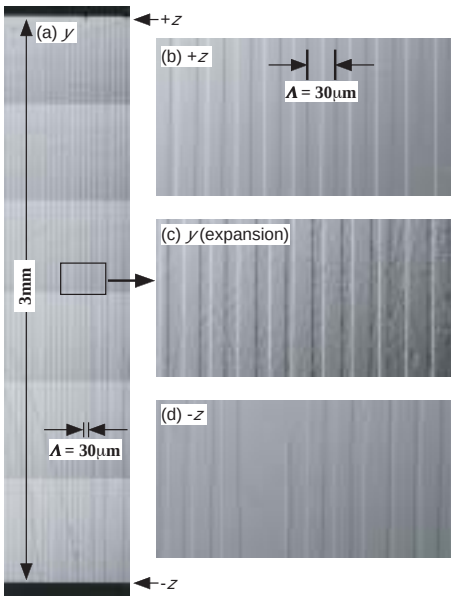

Figure 2.

VIII-B-8 Energy Transfer Processes of Nd^{3+} in Y_2O_3 Ceramic

LUPEI, Aurelia[1]; LUPEI, Voicu[1]; TAIRA, Takunori; SATO, Yoichi; IKESUE, Akio[2]; GHEORGHE, Cristian[1]
([1]Inst. Atomic Phys.; [2]JFCC)

[*J. Lumin.* **102-103**, 72–76 (2003)]

The paper presents spectroscopic and energy transfer results from the investigation of Nd^{3+}:Y_2O_3 transparent ceramics, as a new variant of a laser material. The positions of main Nd^{3+} lines (N) in ceramic Nd^{3+}:Y_2O_3, at low concentrations, are identical to those reported for single crystals. The absence of any other spectral satellites than those corresponding to Nd^{3+} pairs (M) as well as the relative intensity of M lines, show that no structural defects are present in the crystalline lattice of ceramic grains and that the distribution of Nd^{3+} ions at the available lattice sites is random. Thus, from spectroscopic and microstructural point of view, the ceramic Nd^{3+}:Y_2O_3 materials are similar to single crystals. At least two satellite lines were observed in high resolution absorption spectra and assigned to pairs of identical Nd^{3+} centers at nearest distances, C_2–C_2 pairs (8 sites at distances smaller than 4 Å) and dissimilar Nd^{3+} centers ,

C_2–C_{3i} pairs (4 sites at distances smaller than 4 Å).

The global emission decays of $^4F_{3/2}$ Nd^{3+} level at 300 K show strong concentration dependence. The decays for concentrations up to ~ 3 at% present a complex non-exponential behavior, that is interpreted in terms of a cross-relaxation process involving at least two types of interactions: a short range—probably superexchange—connected with interaction within near neighbor pairs and dipole–dipole and a migration term. Though the system contains two types of Nd^{3+} sites, no energy transfer or cross-relaxation to C_{3i} sites is considered for low concentrations since no magnetic dipole allowed transitions are involved in these processes. The efficient energy transfer for low concentrations (dipole-dipole microparameter $C_{DA} \sim 3.7 \times 10^{-39}$ cm^6 s^{-1} is ~ 20 times larger than that for Nd^{3+} in YAG[1]) and the additional transfer mechanisms at higher concentrations determines a strong drop of emission quantum efficiency with concentration and restricts the range of Nd^{3+} concentration in Y_2O_3 useful for laser emission to the range of ~ 1 at%.

Reference

1) V. Lupei, A. Lupei, S. Georgescu, T. Taira, Y. Sato and A. Ikesue, *Phys. Rev. B* **61**, 092102 (2001).

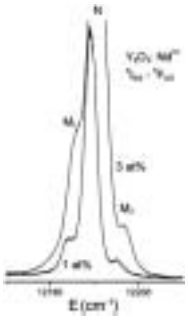

Figure 1. The absorption spectra corresponding to $^4I_{9/2} \rightarrow {}^4F_{5/2}$ (1) transition of Nd^{3+} in Y_2O_3 ceramic for 1 and 3 at%.

VIII-B-9 Second-Harmonic Nonlinear Mirror CW Mode Locking in Yb:YAG Microchip Lasers

SAIKAWA, Jiro; TAIRA, Takunori

[*Jpn. J. Appl. Phys.* **42**, L649 (2003)]

In recent years there has been great interest in sub-picosecond diode-pumped solid-state lasers with multi-watt average powers. Yb:YAG is the candidate for high power sub-picosecond lasers because it has wide emission bandwidth and large thermal conductivity. For high power sub-picosecond mode locked lasers, our approach is the second harmonic nonlinear mirror mode locking (NLM) technique. This technique is based on the second harmonic generation (SHG); thus it has no absorption losses and does not require interferometric cavity length control. In this paper we report the demonstration of a cw-pumped Yb:YAG laser that is passive mode-locked by the nonlinear mirror technique; the possibility to obtain high power sub-picosecond Yb:YAG lasers under diode laser pumping is discussed.

The experimental setup of NLM mode locked Yb:YAG laser is shown in Figure 1. A 15-at.% Yb:YAG chip (1 mm thickness) was used; the Yb:YAG crystal was sandwiched between two undoped YAG plates and is contact with a copper heatsink (~ 20 °C). The cavity length is ~ 2 m and excepting the output coupler M6, the other cavity mirrors were coated as high reflectivity around 1030 nm; moreover, the mirrors M5 and M6 were high reflectivity coated at the SH wavelength. Two LBO crystals (10 mm and 5-mm length) that were cut for type-I temperature tuned non-critical phase matching and antireflection coated for both the fundamental and SH wavelength were used. The LBO crystal was inserted into an oven whose temperature was controlled with 0.1 °C accuracy. The nonlinear mirror was composed of the LBO crystal and the output coupler M6.

In the mode locking operation (under phase-matching), the laser jumped from cw operation to self-start cw mode locking operation. The pulse duration was measured to 9 ps (5mm-LBO). This limitation of pulse width was due to bandwidth of nonlinear mirror. The pulse repetition rate was 82 MHz, and a maximum average power of 900 mW and an optical conversion efficiency of 54% were obtained.

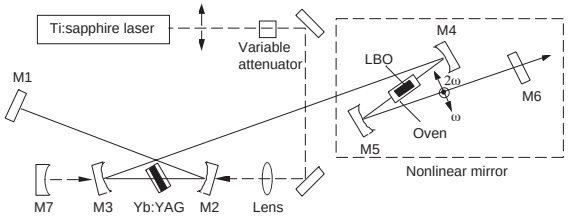

Figure 1. The cavity set up of NLM mode-locked Yb:YAG laser.